INTERNATIONAL JOURNAL FOR NUMERICAL METHODS IN FLUIDS
Int. J. Numer. Meth. Fluids 2003; **42**:79–88 (DOI: 10.1002/fld.533)

A novel fully-implicit finite volume method applied to the lid-driven cavity problem. Part II. Linear stability analysis

Mehmet Sahin and Robert G. Owens*,†

FSTI-ISE-LMF, Ecole Polytechnique Fédérale de Lausanne, CH 1015 Lausanne, Switzerland

SUMMARY

A novel finite volume method, described in Part I of this paper (Sahin and Owens, *Int. J. Numer. Meth. Fluids* 2003; **42**:57–77), is applied in the linear stability analysis of a lid-driven cavity flow in a square enclosure. A combination of Arnoldi's method and extrapolation to zero mesh size allows us to determine the first critical Reynolds number at which Hopf bifurcation takes place. The extreme sensitivity of the predicted critical Reynolds number to the accuracy of the method and to the treatment of the singularity points is noted. Results are compared with those in the literature and are in very good agreement. Copyright © 2003 John Wiley & Sons, Ltd.

KEY WORDS: implicit finite volume methods; lid-driven cavity flow; linear stability

1. INTRODUCTION

The problem of lid-driven cavity flow of a Newtonian fluid is a particularly alluring one for the computational fluid dynamicist in view not only of the simplicity of the flow geometry—making for easy meshing—but also the richness of the fluid mechanical phenomena realizable at various Reynolds numbers: corner eddies, flow bifurcations and transition to turbulence, amongst them. For a detailed but readable treatise of the fluid mechanics in the driven cavity, the reader is referred to that of Shankar and Deshpande [1].

In the literature, however, in contrast with the proliferation of papers evaluating the performance of computational algorithms for the incompressible Navier–Stokes equations in the lid-driven cavity problem, only a handful of papers consider the question of the linear stability of this flow. In conformity with expectation, given the reduced severity of the lid-wall

* Correspondence to: R. G. Owens, FSTI-ISE-LMF, Ecole Polytechnique Fédérale de Lausanne, CH 1015 Lausanne, Switzerland.
† E-mail: robert.owens@effl.ch

Contract/grant sponsor: Swiss National Science Foundation; contract/grant number: 21-61865.00

Received February 2002
Revised 20 August 2002

singularities, the regularized lid-driven cavity problem is more stable than in the unregularized case. Taking a tangential velocity profile $u(x) = 16x^2(1-x)^2$ along the lid $\{(x,1):\ 0 \leqslant x \leqslant 1\}$ in the two-dimensional case, Shen [2] was able to compute steady solutions for Reynolds numbers up to 10 000. However, taking the steady solution at $Re = 10\,000$ as initial data, a periodic solution was found at $Re = 10\,500$; his Chebyshev code thus indicating the presence of a Hopf bifurcation somewhere in the interval $[10\,000, 10\,500]$. Another bifurcation was believed to occur at a critical Reynolds number in the interval $[15\,000, 15\,500]$ with the flow becoming two-periodic. Both Batoul *et al.* [3] and Botella [4] confirmed Shen's observation of a Hopf bifurcation at a critical Reynolds number in the range $[10\,000, 10\,500]$ by computing a solution to the same regularized problem at a Reynolds number of 10 300 starting from a steady solution at $Re = 10\,000$. In both cases a periodic flow was reached, the period based on the kinetic energy being 3.03 for Batoul *et al.* and 3.0275 for Botella. A finite element method, in combination with the simultaneous inverse iteration method of Jennings [5], was used by Fortin *et al.* [6] in 1997 to compute a subset of the eigenvalues for the linear stability problem. The first critical eigenvalue was found at a Reynolds number of approximately 10 255, consistent with the results of Shen [2]. However, the calculated fundamental frequency for the periodic flow was $f \approx 0.331$; rather different from that of Shen. Recent computations by Leriche and Deville [7] for the same regularized problem at a Reynolds number of 10 500 yielded a periodic solution with fundamental frequency $f \approx 0.330$, in good agreement with previous results. As a case in between the regularized lid profile of Shen [2] and the unregularized constant lid-velocity $u(x) = 1$, Leriche and Deville [7] also considered the high-order polynomial approximation $u(x) = (1 - x^{14})^2$ where the lid was now defined to be $\{(x,1):\ -1 \leqslant x \leqslant 1\}$. A direct numerical simulation by the authors with their Chebyshev-τ method at $Re = 8500$ gave rise to a periodic solution with fundamental frequency 0.434 and a kinetic energy signal exhibiting a period of 2.305. Thus the critical Reynolds number had already been exceeded.

The solution to the high-order regularized problem obtained by Leriche and Deville [7] was in good agreement with the results of computations by other authors on the unregularized problem: in two recent papers Pan and Glowinski [8] and Kupferman [9] both obtained limit cycle solutions at $Re = 8500$ with the kinetic energy period of Kupferman's calculations equal to 2.5 approximately. The results of Botella and Peyret [10] indicated a kinetic energy period of 2.246 at a Reynolds number of 9000.

It would seem that very few authors have wished to commit themselves to stating a value for the first critical Reynolds number Re_{crit} for lid-driven cavity flow. The reasons for this would certainly include the cost of determining the Hopf bifurcation point, as well as the computational difficulties associated with its accurate evaluation. For a detailed consideration of these points we refer the reader to the discussion by Poliashenko and Aidun [11] where three types of strategy (time evolution, test function and direct approaches) for analyzing the stability of equilibrium states and their bifurcation are presented. Additionally, we should add that the computation of the critical Reynolds number is a stringent test of the quality of the numerics, and more so, possibly, than that which is involved in comparisons of various variable values (stream function, velocity components, etc.). This is borne out in the numerical results to be presented in this paper, but the magnification brought to bear by critical Reynolds number calculations on the differences between one scheme and another has been seen already in the literature, in the comparison performed by Gervais *et al.* [12], for example, of differing finite element dicretizations for lid-driven flow. Interestingly in this paper the introduction of

SUPG-type stabilization via an enrichment of the velocity trial space with cubic bubbles led to an over diffusive scheme and a critical Reynolds number (9200) which was well outside the range predicted by the second-order finite elements tested. Thus streamline upwinded methods, although enhancing stability, may compromise accuracy to the point that the predicted critical Reynolds numbers are of questionable value. No upwinding or artificial viscosity model is used in the finite volume scheme described in this paper.

Although, at the time of writing, the first critical Reynolds number for the square two-dimensional lid-driven cavity problem is still not known, a consensus seems to be emerging that $Re_{\text{crit}} \approx 8000$. Poliashenko and Aidun [11] used a direct method for the computation of the critical Reynolds number by augmenting the generalized eigenvalue problem with normalizing conditions on the real and imaginary parts of the eigenvectors. Re_{crit} was then determined as part of the solution of the enlarged system and on their finest mesh a value of $Re_{\text{crit}} \approx 7763$ was predicted with a fundamental frequency of about 2.863. Excellent agreement with the Poliashenko and Aidun value was obtained by Cazemier *et al.* [13]. The authors employed a proper orthogonal decomposition (POD) of the flow in a square cavity at $Re = 22\,000$ in order to construct a low-dimensional model for driven cavity flows. Only the first 80 POD modes were used but these were shown to capture 95% of the fluctuating kinetic energy. By linear extrapolation of the real parts of the most dangerous eigenvalues computed using the 80 dimensional model, Cazemier *et al.* predicted a critical Reynolds number of 7819, just 0.7% greater than that of Poliashenko and Aidun. A second-order finite element method and the iteration method of Jennings [5], enabled Fortin *et al.* [6] to conclude that the critical Reynolds number was around 8000. Since the most dangerous eigenvalues crossed the imaginary axis as a complex conjugate pair, and since the amplitude of the fundamental frequency at the point of bifurcation was very small (9×10^{-5}) in their computations, sufficient evidence had been amassed by Fortin *et al.* to support the conclusion that the bifurcation is a supercritical Hopf bifurcation. From the scanty evidence available in the literature, two-dimensional driven cavity flow in non-square (but still rectangular) domains, or subject to three-dimensional infinitesimal perturbations, is less stable than that in square cavities with two-dimensional disturbances. See References [11, 14].

The present paper is organized as follows: in Section 2 we begin by recalling the Navier–Stokes equations and proceed to consider the behaviour with time of infinitesimal perturbations. The implicit finite volume scheme introduced in Part I of this paper [15] is used to discretize the generalized eigenvalue problem (GEVP). This method involves multiplication of the primitive variable-based momentum equation with the vector normal to a control volume boundary, thus eliminating the pressure term from the governing equations when the control volume boundary integral is evaluated. The algebraic system for the nodal values of the eigenfunctions is derived. In Section 2 we also explain how we will use the method of Arnoldi [16, 17] for the accurate determination of the most dangerous eigenvalues that appear when the steady base flow is subjected to two-dimensional infinitesimal perturbations. Section 3 is then dedicated to a discussion of the numerical results. Computations are performed on three meshes of increasing mesh density; with the finest of which are associated 132 098 degrees of freedom. For the linear stability calculations, different size Krylov spaces in Arnoldi's method are chosen to confirm the good accuracy of the eigenspectrum near the imaginary axis. Linear interpolation of the real parts of the most dangerous eigenvalues for the three meshes and extrapolation to zero mesh size of the curve fitted to the Re_{crit}-control volume size data, give us a predicted Re_{crit} of 8031.93—a 0.40% difference from that of Fortin

et al. [6], 2.72% difference from that of Cazemier *et al*. [13] and 3.46% difference from that of Poliashenko and Aidun [11].

2. LINEAR STABILITY ANALYSIS

The incompressible unsteady Navier–Stokes equations may be written in dimensionless form over some domain $\Omega \subset \mathbb{R}^2$ as

$$\nabla \cdot \mathbf{u} = 0 \tag{1}$$

$$\frac{\partial \mathbf{u}}{\partial t} + (\mathbf{u} \cdot \nabla)\mathbf{u} = -\nabla p + \frac{1}{Re}\nabla^2 \mathbf{u} \tag{2}$$

where, in the usual notation, $\mathbf{u} = (u, v)$ denotes the velocity field, p the pressure and Re is a Reynolds number.

In Part I of this paper we showed that integration of (1) over a finite volume $\Omega_{i,j}$ and multiplication of Equation (2) with a vector normal to the boundary $\partial\Omega_{i,j}$ of $\Omega_{i,j}$, followed by integration around $\partial\Omega_{i,j}$ led to

$$\oint_{\partial\Omega_{i,j}} \mathbf{n} \cdot \mathbf{u}\, \mathrm{d}s = 0 \tag{3}$$

and

$$\oint_{\partial\Omega_{i,j}} \mathbf{n} \times \left[\frac{\partial \mathbf{u}}{\partial t} + (\nabla \times \mathbf{u}) \times \mathbf{u} + \frac{1}{Re}\nabla \times (\nabla \times \mathbf{u})\right] \mathrm{d}s = \mathbf{0} \tag{4}$$

respectively. To study the linear stability of the steady base flow velocity $\mathbf{u} = \mathbf{U}$, computed using Newton's method as described in Part I of this paper [15], we consider the behaviour with time of the infinitesimally perturbed flow

$$\mathbf{u} = \mathbf{U}(\mathbf{x}) + \mathbf{v}(\mathbf{x}) \exp(\sigma t) \tag{5}$$

Inserting (5) into (3) and (4), assuming $\mathbf{U}$ to be an exact solution to the steady Navier–Stokes equations and neglecting quadratic terms in $\mathbf{v}$ we get

$$\oint_{\partial\Omega_{i,j}} \mathbf{n} \cdot \mathbf{v}\, \mathrm{d}s = 0 \tag{6}$$

and

$$\oint_{\partial\Omega_{i,j}} \mathbf{n} \times \left[(\nabla \times \mathbf{U}) \times \mathbf{v} + (\nabla \times \mathbf{v}) \times \mathbf{U} + \frac{1}{Re}\nabla \times (\nabla \times \mathbf{v})\right] \mathrm{d}s = -\sigma \oint_{\partial\Omega_{i,j}} \mathbf{n} \times \mathbf{v}\, \mathrm{d}s \tag{7}$$

The evaluation of the line integrals appearing in (6) and (7) follows very closely the ideas employed for the solution of the steady equations of linear momentum and conservation of mass described in Section 2.2 of Part I [15]: the line integrals are computed using the mid-point rule and in (7) a perturbation vorticity vector $\boldsymbol{\omega} = \nabla \times \mathbf{v}$ is defined at the centre of each finite volume. Face values of vorticity are then determined from simple averages of the

Table I. Pseudo-code for Arnoldi's method. $h_{i,j}$ is the (i,j)th element of an upper Hessenberg matrix H. The vectors $\mathbf{x}_1, \mathbf{x}_2, \ldots, \mathbf{x}_m$ form an orthonormal system by construction (modified Gram-Schmidt algorithm).

$$
\begin{array}{l}
\mathbf{x}_1 = \frac{\mathbf{x}}{\|\mathbf{x}\|_2} \\
\text{for } j = 1, 2, \ldots, m \text{ do} \\
\quad \mathbf{w} = A^{-1} M \mathbf{x}_j \\
\quad\quad \text{for } i = 1, 2, \ldots, j \text{ do} \\
\quad\quad\quad h_{i,j} = \mathbf{w} \cdot \mathbf{x}_i \\
\quad\quad\quad \mathbf{w} = \mathbf{w} - h_{i,j} \mathbf{x}_i \\
\quad\quad \text{end for} \\
\quad h_{j+1,j} = \|\mathbf{w}\|_2 \\
\quad \mathbf{x}_{j+1} = \mathbf{w} / h_{j+1,j} \\
\text{end for}
\end{array}
$$

cell-centred values in the cells either side of the face in question. The end result of following this procedure for the evaluation of (6) and (7) is a discrete algebraic system for the nodal values of $\mathbf{v}$ of the form

$$A\mathbf{x} = \sigma M \mathbf{x} \tag{8}$$

A being almost the same (by construction) as the coefficient matrix arising from the discretization of the continuity equation and momentum equation, described in Section 2.2 of Reference [15], the sole difference being that nodal values of $\mathbf{u}^n$ (the nth Newton iterative value of velocity) are now replaced with the corresponding nodal values of $\mathbf{U}$. The matrix M in (8) is block bi-diagonal. The GEVP (8) is solved by applying the Arnoldi method [16, 17] to the equivalent system

$$C\mathbf{x} = \mu \mathbf{x} \tag{9}$$

where $C = A^{-1}M$ and $\mu = \sigma^{-1}$. A pseudo-code form of Arnoldi's method for a Krylov space of dimension m is given in Table I. The procedure leads to the construction of an $m \times m$ upper Hessenberg matrix H whose eigenvalues (the so-called Ritz values $\hat{\mu}$) are approximations to eigenvalues μ of C. Since Arnoldi's method results in fastest convergence to the *extremal* eigenvalues of C, the best resolution of the eigenspectrum will be for eigenvalues σ of the pencil $A - \sigma M$ nearest the origin. In fact although—as will be seen in the numerical results—the imaginary axis is first crossed by a complex conjugate *pair* of eigenvalues, these are supposed to be adequately approximated by the reciprocals $\hat{\mu}^{-1}$ of the corresponding Ritz values. Incorporating a complex shift [18], although desirable from the point of view of accuracy, would necessitate working in complex arithmetic and increase significantly the computational cost. The Ritz values of H are computed by using the Intel Math Kernel Library which uses a multishift form of the upper Hessenberg QR algorithm.

3. NUMERICAL RESULTS

The use of the steady Navier–Stokes solver described in Part I of this paper [15] and Arnoldi's method (see Section 2) enable us to compute the first critical Reynolds number at which a Hopf bifurcation occurs. This is done by inspecting the real part of the most dangerous reciprocal Ritz value pair $\hat{\mu}_{1,2}^{-1}$. For any given mesh this is done for a variety of Krylov space dimensions m and the process repeated over a range of Reynolds numbers until the real part of the aforementioned reciprocal Ritz values is positive. For reasonable accuracy the incremental step size in Reynolds number during the search for a Hopf bifurcation should be kept as small as possible. The critical Reynolds number on a given mesh is then determined by a linear interpolation between the last point on the graph of $\Re(\hat{\mu}_{1,2}^{-1})$ vs Re having $\Re(\hat{\mu}_{1,2}^{-1})<0$ and the first with $\Re(\hat{\mu}_{1,2}^{-1})>0$. For the finest mesh the critical Reynolds number is determined to be $Re=8069.76$. The computed streamlines and vorticity contours at this Reynolds number are given in Figure 1. The complete reciprocal Ritz value spectrum computed at this Reynolds number with a Krylov subspace dimension $m=250$ is presented in Figure 2 and the values of the first ten leading eigenvalues is given in Table II for further comparison. For the eigenspectrum we observe good agreement with the results of Fortin *et al.* [6]. The imaginary part of the leading eigenvalue is computed on mesh M3 to be 2.8251 which is also in good agreement with the corresponding value (2.8356) of Fortin *et al.* [6] bearing in mind the fact that the two imaginary parts (ours and that of Fortin *et al.*) are computed at rather different Reynolds numbers. The critical Reynolds numbers are also computed with meshes M1 and M2. The precise critical values are tabulated in Table III. The Krylov space dimension m corresponding to mesh M3 and shown in the third column is the largest that we can afford with the current PC. Columns 4 and 5 detail, respectively, the real and absolute value of the

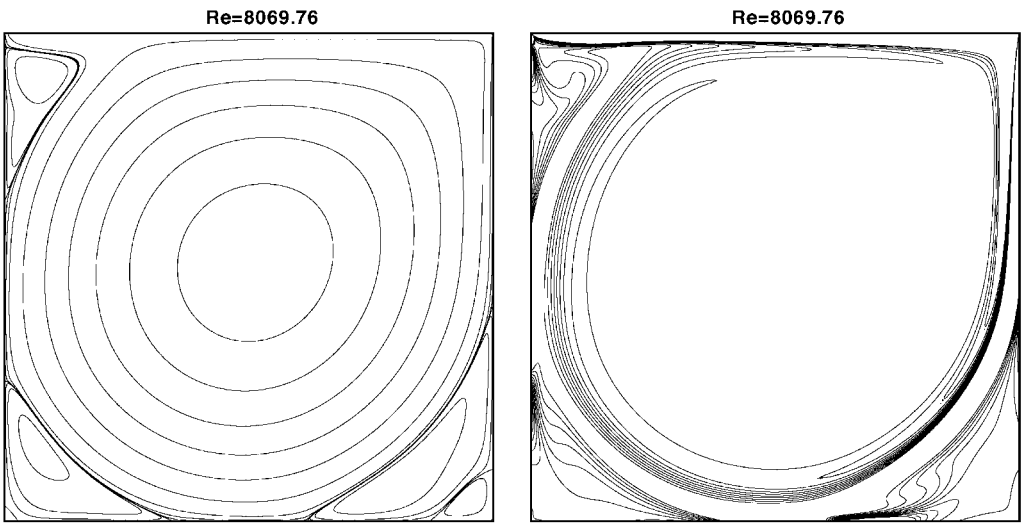

Figure 1. Streamlines and vorticity contours computed at critical Reynolds number of 8069.76 with mesh M3. The stream function contour levels shown are −0.11, −0.09, −0.07, −0.05, −0.03, −0.01, −0.001, −0.0001, −0.00001, 0.0, 0.00001, 0.0001, 0.001 and 0.01. Contour levels for the vorticity plot are −5.0, −4.0, −3.0, −2.0, −1.0, 0.0, 1.0, 2.0, 3.0, 4.0 and 5.0.

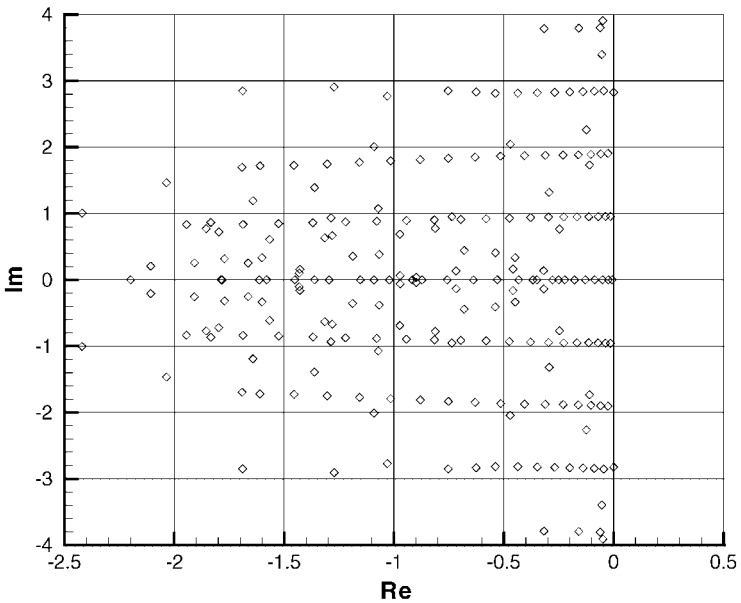

Figure 2. Reciprocal Ritz values computed on mesh M3 at $Re = 8069.76$ with Krylov space dimension $m = 250$.

Table II. The first 10 reciprocal Ritz values computed on mesh M3 at $Re = 8069.76$.

n	σ_R	σ_I
1	-1.9025×10^{-7}	± 2.8251
2	-7.3257×10^{-3}	0.0000
3	-1.4161×10^{-2}	± 0.9576
4	-2.4387×10^{-2}	0.0000
5	-2.5916×10^{-2}	± 1.9062
6	-3.7116×10^{-2}	± 0.9551
7	-4.5205×10^{-2}	± 2.8520
8	-4.9557×10^{-2}	± 3.9063
9	-5.0851×10^{-2}	0.0000
10	-5.3889×10^{-2}	± 3.3969

imaginary parts (σ_R and σ_I) of the most dangerous pair of reciprocal Ritz values computed at the interpolated critical Reynolds number. We note from the spread of values in the second column of Table III that critical Reynolds number calculations would seem to be a much more discerning measure of solution accuracy than, for example, the streamline or velocity values that are habitually presented in the literature (see Table II of Reference [15]). Thankfully, for any given mesh, σ_R was not found to be an overly sensitive function of m. As an example, in Table IV we show the ten reciprocal Ritz values having largest real parts, as computed on mesh M1 with Krylov spaces of dimensions $m = 250$ and 500. Very good agreement in both the real imaginary parts of these leading reciprocal Ritz values can be seen.

Table III. Computed critical Reynolds numbers $Re_c(h)$ for meshes M1 to M3. The final value of $Re_c(h)$ is the extrapolated value Re_c.

Mesh	$Re_c(h)$	m	σ_R	σ_I
M1	8244.55	250	-5.9487×10^{-8}	± 2.8315
M2	8109.38	250	-1.7769×10^{-7}	± 2.8256
M3	8069.76	250	-1.9025×10^{-7}	± 2.8251
Extrap	8031.92	—	—	—

Table IV. 10 leading reciprocal Ritz values computed at $Re = 8244.55$ on mesh M1 with Krylov subspace dimensions $m = 250$ and 500.

$m = 250$		$m = 500$	
σ_R	σ_I	σ_R	σ_I
-5.9487×10^{-8}	± 2.8315	-4.7800×10^{-8}	± 2.8315
-7.0198×10^{-3}	0.0000	-7.0198×10^{-3}	0.0000
-1.4154×10^{-2}	± 0.9643	-1.4154×10^{-2}	± 0.9643
-2.3571×10^{-2}	0.0000	-2.3571×10^{-2}	0.0000
-2.4539×10^{-2}	± 1.9159	-2.4539×10^{-2}	± 1.9160
-3.6512×10^{-2}	± 0.9593	-3.6512×10^{-2}	± 0.9593
-4.0236×10^{-2}	± 2.8600	-4.0234×10^{-2}	± 2.8600
-4.4007×10^{-2}	± 3.8954	-4.4746×10^{-2}	± 3.8951
-4.8049×10^{-2}	± 3.3908	-4.8055×10^{-2}	± 3.3908
-4.9438×10^{-2}	0.0000	-4.9438×10^{-2}	0.0000

In order to estimate a value for the critical Reynolds number based on a zero mesh size (Re_c, say), a relationship was sought of the form

$$Re_c(h) = Re_c + ch^p \tag{10}$$

between Re_c and the critical Reynolds number $Re_c(h)$ computed on a mesh having average cell length h. Thus, identifying an average cell length h with mesh $M1$, we have

$$\begin{aligned} \frac{Re_c(h) - Re_c(2h/3)}{Re_c(h) - Re_c(h/2)} &= \frac{(Re_c(h) - Re_c) - (Re_c(2h/3) - Re_c)}{(Re_c(h) - Re_c) - (Re_c(h/2) - Re_c)} \\ &= \frac{ch^p - c(\frac{2}{3})^p h^p}{ch^p - c(\frac{1}{2})^p h^p} \\ &= \frac{1 - (\frac{2}{3})^p}{1 - (\frac{1}{2})^p} = \frac{8244.55 - 8109.38}{8244.55 - 8069.76} \end{aligned} \tag{11}$$

which yields a solution $p \approx 2.4906$.

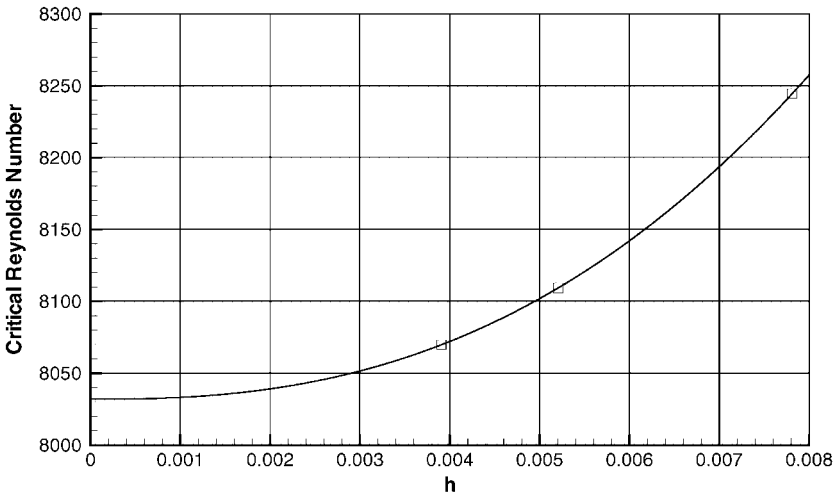

Figure 3. Critical Reynolds number $Re_c(h)$ plotted as a function of the average finite volume cell size h. The equation for the continuous curve drawn through the three data points is given by (10).

Now

$$\frac{Re_c - Re_c(h)}{Re_c - Re_c(h/2)} = \frac{ch^p}{c(\frac{1}{2})^p h^p} = 2^p \tag{12}$$

Therefore, rearranging, we get

$$Re_c = \frac{1}{2^p - 1}[2^p Re_c(h/2) - Re_c(h)] \tag{13}$$

and with p as calculated above we get $Re_c \approx 8031.93$. In Figure 3 we present a graph of both the interpolatory function given in Equation (10) and the data points corresponding to the critical values of the Reynolds number computed with the three meshes M1–M3. The extrapolated result agrees well with the prediction of Fortin *et al.* [6] ($Re_c \approx 8000$), and represents only a 3.46% difference from the value of Re_c calculated by Poliashenko and Aidun [11] ($Re_c = 7763$) and a 2.72% difference from the Re_c value of Cazemier *et al.* [13] ($Re_c = 7819$). Most probably, the introduction of small leaks in the upper corners of the cavity in the present numerical method smooths out the solution and leads to the flow becoming unstable at a slightly larger critical Reynolds number.

4. CONCLUSIONS

In this paper we have presented application of a novel implicit finite volume method to the linear stability analysis of a lid-driven cavity flow. The method is combined with Arnoldi's method for the determination of the linear stability properties. We have obtained a first critical Reynolds number in very good agreement with the few others published to date. We observed that its value is highly sensitive to the accuracy of the method and to the treatment of the singularities. Although eigenvalue calculations are computationally very expensive, the block

banded matrix structure of the coefficient matrix in the GEVP and the use of Arnoldi's method allows us to compute the first 250 eigenvalues using the finest mesh.

ACKNOWLEDGEMENTS

The work of the first author is supported by the Swiss National Science Foundation, grant number 21-61865.00

REFERENCES

1. Shankar PN, Deshpande MD. Fluid mechanics in the driven cavity. *Annual Review of Fluid Mechanics* 2000; **32**:93–136.
2. Shen J. Hopf bifurcation of the unsteady regularized driven cavity flow. *Journal of Computational Physics* 1991; **95**(1):228–245.
3. Batoul A, Khallouf H, Labrosse G. Une méthode de résolution directe (pseudo-spectrale) du problème de Stokes 2D/3D instationnaire. Application à la cavité entrainée carrée. *Comptes Rendus de l'Académie des Sciences de Paris* 1994; **319**(12):1455–1461.
4. Botella O. On the solution of the Navier-Stokes equations using Chebyshev projection schemes with third-order accuracy in time. *Computers & Fluids* 1997; **26**(2):107–116.
5. Jennings A. *Matrix Computation for Engineers and Scientists*. Wiley: London, 1977.
6. Fortin A, Jardak M, Gervais JJ, Pierre R. Localization of Hopf bifurcations in fluid flow problems. *International Journal for Numerical Methods in Fluids* 1997; **24**(11):1185–1210.
7. Leriche E, Deville MO. A Uzawa-type pressure solver for the Lanczos-τ-Chebyshev spectral method. *Computers & Fluids* 2003; submitted.
8. Pan TW, Glowinski R. A projection/wave-like equation method for the numerical simulation of incompressible viscous fluid flow modeled by the Navier-Stokes equations. *Computational Fluid Dynamics Journal* 2000; **9**(2):28–42.
9. Kupferman R. A central-difference scheme for a pure stream function formulation of incompressible viscous flow. *SIAM Journal on Scientific Computing* 2001; **23**(1):1–18.
10. Botella O, Peyret R. Computing singular solutions of the Navier-Stokes equations with the Chebyshev-collocation method. *International Journal for Numerical Methods in Fluids* 2001; **36**(2):125–163.
11. Poliashenko M, Aidun CK. A direct method for computation of simple bifurcations. *Journal of Computational Physics* 1995; **121**(2):246–260.
12. Gervais JJ, Lemelin D, Pierre R. Some experiments with stability analysis of discrete incompressible flows in the lid-driven cavity. *International Journal for Numerical Methods in Fluids* 1997; **24**(5):477–492.
13. Cazemier W, Verstappen RWCP, Veldman AEP. Proper orthogonal decomposition and low-dimensional models for driven cavity flows. *Physics of Fluids* 1998; **10**(7):1685–1699.
14. Goodrich JW, Gustafson K, Halasi K. Hopf bifurcation in the driven cavity. *Journal of Computational Physics* 1990; **90**(1):219–261.
15. Sahin M, Owens RG. A novel fully-implicit finite volume method applied to the lid-driven cavity problem. Part I. High Reynolds number flow calculations. *International Journal for Numerical Methods in Fluids* 2003; **42**:57–77.
16. Arnoldi WE. The principle of minimized iterations in the solution of the matrix eigenvalue problem. *Quarterly of Applied Mathematics* 1951; **9**:17–29.
17. Saad Y. Variations on Arnoldi's method for computing eigenelements of large unsymmetric matrices. *Linear Algebra and its Applications* 1980; **34**:269–295.
18. Natarajan R. An Arnoldi-based iterative scheme for nonsymmetric matrix pencils arising in finite element stability problems. *Journal of Computational Physics* 1992; **100**(1):128–142.

